Probing Domain Mobility in a Flavocytochrome[†,‡]

Emma L. Rothery,[§] Christopher G. Mowat,[§,||] Caroline S. Miles,[||] Sarah Mott,[||] Malcolm D. Walkinshaw,[||] Graeme A. Reid,[||] and Stephen K. Chapman*[,§]

School of Chemistry, University of Edinburgh, West Mains Road, Edinburgh, EH9 3JJ, United Kingdom, and Institute of Cell and Molecular Biology, University of Edinburgh, Mayfield Road, Edinburgh, EH9 3JR, United Kingdom

Received December 19, 2003; Revised Manuscript Received February 13, 2004

ABSTRACT: The crystal structures of various different members of the family of fumarate reductases and succinate dehydrogenases have allowed the identification of a mobile clamp (or capping) domain [e.g., Taylor, P., Pealing, S. L., Reid, G. A., Chapman, S. K., and Walkinshaw, M. D. (1999) *Nat. Struct. Biol. 6*, 1108−1112], which has been proposed to be involved in regulating accessibility of the active site to substrate. To investigate this, we have constructed the A251C:S430C double mutant form of the soluble flavocytochrome c_3 fumarate reductase from *Shewanella frigidimarina*, to introduce an interdomain disulfide bond between the FAD-binding and clamp domains of the enzyme, thus restricting relative mobility between the two. Here, we describe the kinetic and crystallographic analysis of this double mutant enzyme. The 1.6 Å resolution crystal structure of the A251C:S430C enzyme under oxidizing conditions reveals the formation of a disulfide bond, while Ellman analysis confirms its presence in the enzyme in solution. Kinetic analyses with the enzyme in both the nonbridged (free thiol) and the disulfide-bridged states indicate a slight decrease in the rate of fumarate reduction when the disulfide bridge is present, while solvent−kinetic−isotope studies indicate that in both wild-type and mutant enzymes the reaction is rate limited by proton and/or hydride transfer during catalysis. The limited effects of the inhibition of clamp domain mobility upon the catalytic reaction would indicate that such mobility is not essential for the regulation of substrate access or product release.

During anaerobic respiration, many bacteria produce a fumarate reductase, which enables the use of fumarate as a terminal electron acceptor. In the majority of organisms, this enzyme is a membrane-bound complex, closely related to succinate dehydrogenase, that uses iron−sulfur centers and FAD[1] as cofactors (*1*, *2*). However, *Shewanella* species contain a soluble periplasmic tetraheme FAD-containing fumarate reductase known as flavocytochrome c_3 (*3*). Crystal structures are available for several members of the fumarate reductase/succinate dehydrogenase family of enzymes, including the fumarate reductase complexes from *Escherichia coli* (*4*; PDB ID 1L0V) and *Wolinella succinogenes* (*5*, *6*; PDB IDs 1QLA, 1QLB, 1E7P), the succinate dehydrogenase complex from *E. coli* (*7*; PDB ID 1NEK), and the soluble fumarate reductases from *Shewanella frigidimarina* NCIMB400 (*8*; PDB ID 1QJD and *9*; PDB ID 1Q08) and *Shewanella oneidensis* MR-1 (*10*; PDB IDs 1D4C, 1D4D, 1D4E).

From comparison of these homologous structures, it is clear that the active site for fumarate reduction/succinate dehydrogenation has a common architecture throughout the family, and the important catalytic residues are conserved. This active site comprises residues from both the FAD-binding and clamp, or capping, domains, which have been identified in all of the structures mentioned. What is also clear is that this clamp domain is mobile relative to the FAD-binding domain, as is evidenced by the different positions it assumes in many of the available structures (Figure 1). It has been proposed that the clamp domain may therefore have a role in allowing substrate access to the active site (*5*, *6*, *8*−*10*). To test this, we aimed to introduce a disulfide bond and restrict interdomain mobility. In this paper, we describe the construction and the kinetic and crystallographic characterization of the A251C:S430C double mutant form of flavocytochrome c_3.

MATERIALS AND METHODS

DNA Manipulation, Strains, Media, and Growth. The double mutant enzyme A251C:S430C flavocytochrome c_3 was constructed using the method described by Kunkel and Roberts (*11*) as described previously (*12*, *13*).

Mutagenic oligonucleotides CCAACCGGTGGT*TGT*GGTGTTGGTGC (which substitutes alanine 251 with cysteine) and GTAAGTCACTGT*GT*AAAATTGATAAG (which substitutes serine 430 with cysteine) were used. Mismatched bases are italic.

Screening for the double mutations was carried out by automated sequencing of plasmid DNA on a Perkin-Elmer

[†] This work was supported by the U.K. Biotechnology and Biological Sciences Research Council (BBSRC) and by the Wellcome Trust funded Edinburgh Protein Interaction Centre (EPIC). E.L.R. acknowledges studentship funding from EPSRC. We thank SRS Daresbury for access to synchrotron facilities.

[‡] The atomic coordinates have been deposited in the Protein Data Bank (entry 1Q9I).

* To whom correspondence should be addressed. Tel/Fax: (+44)-131 650 4760. E-mail: S.K.Chapman@ed.ac.uk.

[§] School of Chemistry, University of Edinburgh.

[||] Institute of Cell and Molecular Biology, University of Edinburgh.

[1] Abbreviations: A251C:S430C, alanine251→cysteine, serine430→cysteine double mutation; FAD, flavin adenine dinucleotide; pL, the equivalent of pH in mixed isotope solvents.

10.1021/bi030261w CCC: $27.50
Published on Web 04/06/2004

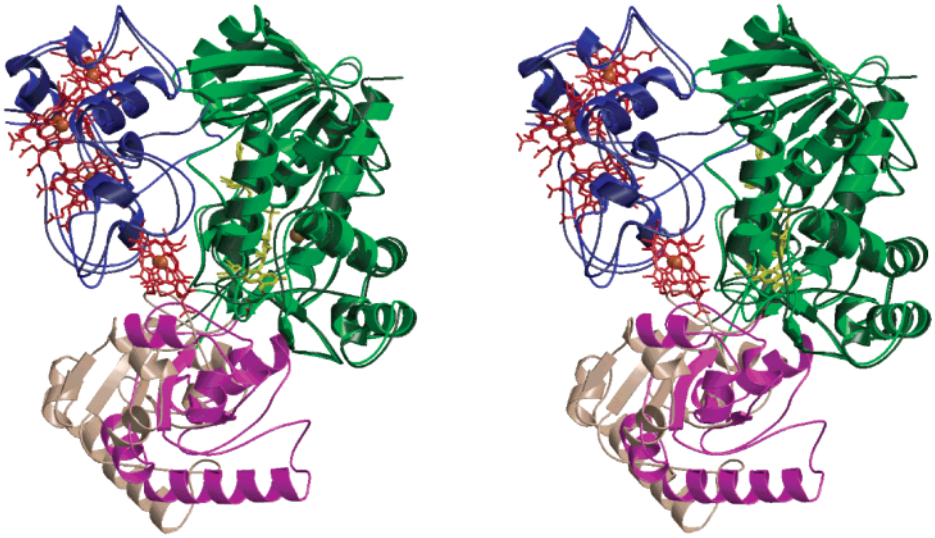

FIGURE 1: Stereoview of the overlaid structures of the substrate-free, fully open [1Q08; (*9*)] and substrate-bound closed [1QJD; (*8*)] forms of *Shewanella* fumarate reductase. The heme domains are colored blue in 1QJD and dark blue in 1Q08, and the FAD-binding domains are green in 1QJD and dark green in 1Q08. The clamp domain is shown in magenta for the closed form and in beige for the open form. This figure was generated using BOBSCRIPT (*26*) and RASTER 3D (*27*).

ABI Prism 377 instrument. The mutated *fccA* coding sequence was fully sequenced to check that no secondary mutations had been introduced.

The modified coding sequence was cloned into the broad host range expression vector pMMB503EH (*14*) on an ~1.8 kbp *Eco*RI-*Hin*dIII fragment to generate pSM130. Expression in the Δ*fccA S. frigidimarina* strain EG301 (*3*) was carried out as described previously (*12*).

Protein Purification and FAD Determination. Wild-type and mutant forms of flavocytochrome c_3 were purified as previously reported (*15*) with an additional purification step using FPLC with a Mono Q column as described by Pealing et al. (*16*). To avoid premature formation of the disulfide bond, all purification buffers were supplemented with 1 mM DTT (dithiothreitol). Protein concentrations were determined using the Soret band absorption coefficient for the reduced enzyme (752.8 mM^{-1} cm^{-1} at 419 nm) (*15*). The FAD content of wild-type and mutant enzymes was determined using the method of Macheroux (*17*), and all steady state rate constants were corrected to account for the percentage of FAD present. Mass spectrometry of proteins was carried out using a Micromass Platform II Electrospray mass spectrometer. Samples were prepared in 5 mM ammonium acetate buffer, pH 6.5, containing 0.1% (v/v) formic acid before being diluted 1:1 with acetonitrile and introduced to the spectrometer via direct infusion. Prior to use, the spectrometer was standardized using horse heart myoglobin.

Ellman Assay. The presence of free cysteine in the protein was determined using the Ellman assay. 2,2′-Dipyridyl disulfide (2-PDS) was reacted with the sulfur of the cysteine residue(s) resulting in cleavage of the central S−S bond within the 2-PDS yielding a protein−pyridyl product and a chromophore. The accumulation of the chromophore was monitored at 343 nm (ϵ_{343} = 8.08 mM^{-1} cm^{-1}) thus quantifying the free cysteine residues in the protein. To prevent air oxidation of any free cysteinyl sulfur, all experiments were performed under a nitrogen atmosphere using a Belle Technology glovebox with O_2 levels maintained at <3 ppm. Stock enzyme was prepared in 100 mM KP_i, pH 7.0, 25 °C, in the presence of 1 mM DTT to ensure that any free cysteines within the protein remained reduced. Immediately prior to experiments, excess DTT was removed by gel filtration (BioRad Econopac 10DG 10 mL column) and the protein eluted from the column was diluted to 10 μM. A 1 mM stock of 2-PDS solution, prepared in ethanol, was diluted 10-fold with the stock 10 μM protein solution in a 1 cm path length quartz cuvette. The change in absorption at 343 nm was observed, the total absorbance change correlated with the quantity of free cysteine in the protein.

For experiments requiring air oxidation of the disulfide bridge, DTT was removed from the protein by gel filtration under anaerobic conditions, with samples being immediately frozen in liquid nitrogen if required. Samples were then dialyzed (12 000 MW cutoff) against 100 mM KP_i, pH 7.0, 25 °C, in the absence of DTT, to allow oxygenated buffer into the sample and oxidative formation of any possible disulfide bonds.

Steady State Kinetic Analysis. The steady state kinetics of fumarate reduction were followed at 25 °C as described by Turner et al. (*18*). The fumarate-dependent reoxidation of reduced methyl viologen was monitored at 600 nm using a Shimadzu UV-PC 1501 spectrophotometer. Methyl viologen was reduced by addition of sodium dithionite until an absorbance of around 1 unit was obtained (corresponding to ~80 μM reduced methyl viologen). A known concentration of enzyme was added, and the reaction was initiated by addition of fumarate (0−1 mM) from a 1 M stock solution. To ensure anaerobicity, the spectrophotometer was housed in a Belle Technology glovebox under a nitrogen atmosphere with the O_2 level maintained below 2 ppm. Assay buffers contained 0.45 M NaCl and 0.2 mM methyl viologen and were adjusted to the appropriate pH values using 0.05 M HCl or NaOH as follows: TrisHCl (pH 7.0−9.0), MES (pH 5.4−6.8), and CHES (pH 8.6−10.0).

Solvent−Kinetic−Isotope Effects. Buffer and substrate solutions were prepared in both D_2O and H_2O, and steady state kinetic assays were performed under saturating fumarate conditions. DCl or NaOD was titrated into the deuterated buffer to correct the pD as required, applying the equation

pD = pH meter reading + 0.4 to correct for the acidity of the pH electrode itself (*19*). The stock protein solution was prepared in H_2O and then concentrated such that the addition of the protonated enzyme solution represented less than 0.05% of the total assay volume. The percentage of D_2O in the buffer was varied between 0 and 100% by a combination of the appropriate proportion of deuterated and protonated buffer in the assay. An equilibration time of ~30 s was allowed before initiation of the assay by addition of fumarate. The rate constants obtained were plotted as a function of D_2O concentration, and a proton inventory was constructed. This was then fitted to a model describing multiple exchangeable hydrogenic sites in reactant and transition states, as described by Schowen and Schowen (*20*). The solvent−kinetic−isotope effect for each enzyme was calculated by the ratio k_H/k_D.

Presteady State Kinetic Analysis. Presteady state kinetic analysis was carried out using an Applied Photophysics SF.17MV stopped-flow spectrophotometer housed within a Belle Technology glovebox under a nitrogen atmosphere with the O_2 level maintained below 2 ppm. The buffer was 0.05 M TrisHCl, pH 7.2, I = 0.5 M (as used in steady state measurements). All experiments were conducted at 25 °C. Stock enzyme solution was reduced by titration with sodium dithionite, and excess reductant was removed via gel filtration (BioRad Econo-pac 10DG 10 mL column) within the anaerobic environment. For samples where the disulfide bridge was required to be open, the stock enzyme was supplemented with 1 mM DTT to prevent oxidation of the cysteine residues. This did not affect the rate of heme oxidation. The fumarate concentration was varied in the range of 1−500 μM, and the course of fumarate-dependent heme oxidation was monitored at 418 nm. Traces obtained were fitted to a double exponential decay, and the rates obtained were plotted as a function of the fumarate concentration. All fitting was done using Origin (Microcal).

Crystallization and Refinement. Crystallization of A251C:S430C flavocytochrome c_3 was carried out by hanging drop vapor diffusion in an air atmosphere at 4 °C in Linbro plates. Crystals were obtained with well solutions comprising 100 mM Tris-HCl buffer (pH 7.8−8.5; measured at 25 °C), 80 mM NaCl, 16−19% PEG 8000, and 10 mM fumarate. Hanging drops (4 μL volume) were prepared by adding 2 μL of 7 mg/mL protein (in 10 mM Tris-HCl, pH 8.5) to 2 μL of well solution. After ~10 days, needles of up to 1 mm × 0.2 mm × 0.2 mm were formed. Crystals were immersed in a solution of 100 mM sodium acetate buffer (pH 6.5), 20% PEG 8000, 10 mM fumarate, and 80 mM NaCl, containing 23% glycerol as a cryoprotectant, prior to mounting in nylon loops and flash-cooling in liquid nitrogen. A data set was collected to 1.6 Å resolution at SRS Daresbury (station 14.2; λ = 0.975 Å) using an ADSC Quantum 4 detector. Crystals were found to belong to space group $P2_1$ with cell dimensions a = 45.290 Å, b = 91.885 Å, c = 78.310 Å, and β = 91.502°. Data processing was carried out using the HKL package (*21*). The wild-type flavocytochrome c_3 structure (1QJD), stripped of water, was used as the initial model for molecular replacement. Electron density fitting was carried out using the program TURBO-FRODO (*22*). Structure refinement was carried out using Refmac5 (*23*). The atomic coordinates have been deposited in the Protein Data Bank, entry 1Q9I.

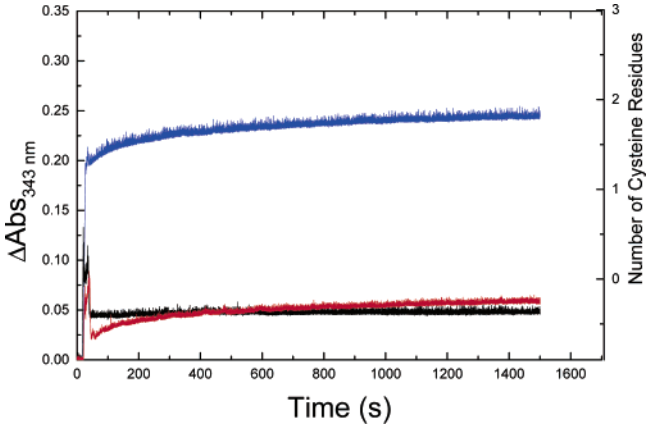

FIGURE 2: Time-dependent traces of the accumulation of the chromophore produced during Ellman assay analysis of flavocytochrome c_3. Shown are traces for the wild-type enzyme (black), the A251C:S430C enzyme with the disulfide bridge (red), and the A251C:S430C with the disulfide open (blue). Data were recorded at 25 °C, pH 7.0, I = 0.1 M, with traces monitored at 343 nm, where ϵ = 8.08 mM^{-1} cm^{-1}.

RESULTS

Mass Spectrometry. Mutations were confirmed by DNA sequencing and electrospray mass spectrometry. Although the sample for protein mass spectrometry was prepared in the presence of DTT, direct infusion of the sample into the instrument required the removal of all nonvolatile buffer components. Buffer exchange to the volatile ammonium acetate buffer was achieved by overnight dialysis of the stock protein (typically 2 mL of 50 μM protein) against 3 × 1 L of 5 mM ammonium acetate. The length of time required and the removal of the DTT under aerobic conditions were most likely sufficient to allow oxidative formation of the disulfide bond. However, the mass difference between the oxidized and the reduced form of the disulfide bond is only 2 Da (due to the loss of two hydrogen atoms in the disulfide-bridged form). Wild-type flavocytochrome c_3 has a mass of 63 033 Da, and the mass difference for the A251C:S430C double mutant form of the enzyme was found to be +45 (±4) Da. In the nonbridged form, the expected mass difference is +44 Da, whereas in the disulfide-bridged form it is +46 Da. The error on the data collected is such that it is impossible to say whether the disulfide bridge is present or absent in the sample, but the presence of both amino acid substitutions is confirmed.

Ellman Assay. Analysis of the amino acid sequence of the wild-type flavocytochrome c_3 reveals there to be eight naturally occurring cysteine residues. These are all found as part of the heme binding motifs for the four *c*-type hemes and are therefore not free to undergo chemical modification. Hence, the only cysteine residues that are detectable via the Ellman assay are those introduced by site-directed mutagenesis.

Accumulation of the chromophore was monitored at 343 nm over a 20 min time scale (Figure 2). The absorbance change is shown on the left-hand axis of Figure 2 while the right-hand axis has been recalculated to show thiol equivalents. Both are shown as a function of time lapsed. Data were collected for the wild-type enzyme in addition to the A251C:S430C mutant with the disulfide bond in both open and bridged forms. Analysis of the A251C:S430C double mutant enzyme in the nonbridged form clearly shows the presence

Table 1: Steady State Kinetic Parameters for Fumarate Reduction in Wild-Type and A251C:S430C Forms of Flavocytochrome c_3 (25 °C, $I = 0.5$ M)

	k_{cat} (s^{-1})			K_M (μM)		
		A251C:S430C			A251C:S430C	
pH	wild-type	S-S red.	S-S ox.	wild-type	S-S red.	S-S ox.
6.0	658 ± 34	226 ± 19	46 ± 9	43 ± 10	20 ± 4	46 ± 4
7.2	509 ± 15	321 ± 12	126 ± 10	25 ± 2	28 ± 4	50 ± 7
7.5	370 ± 10	340 ± 10	149 ± 11	28 ± 3	27 ± 3	50 ± 4
9.0	210 ± 13	224 ± 10	82 ± 7	7 ± 2	29 ± 5	47 ± 6

of two free thiols, in contrast to the wild-type enzyme, which has none. Incubation of the double mutant enzyme in aerobic buffer allowed the oxidative formation of the disulfide bond, and this is reflected in the Ellman assay, resulting in a trace identical to that observed for the wild-type enzyme.

Steady State Kinetic Analysis. The ability of the double mutant enzyme to catalyze the reduction of fumarate was determined over a range of pH values and with the disulfide bond in both its reduced and oxidized forms. The average FAD content for the A251C:S430C double mutant enzyme was found to be 59%, which although slightly lower than the average FAD content of recombinant wild-type flavocytochrome c_3 of 73%, is comparable. All rate constants were corrected for FAD content. Michaelis−Menten plots were constructed by measuring the rate of fumarate reduction at increasing substrate concentrations. The data were then fitted by a least-squares regression analysis to the Michaelis−Menten equation, and the results are shown in Table 1.

Under DTT-reduced conditions, the double substitution of Ala251 and Ser430 to cysteine lowered the k_{cat} of the enzyme to 63% of the wild-type value (at pH 7.2). Although the disulfide bridge is unlikely to be formed under the conditions of the assay, the rate constant is lower than that of the wild-type enzyme. The value of K_M for fumarate binding in the double mutant enzyme is the same as observed in the wild-type enzyme, indicating that substrate binding at the active site is unaffected by the substitutions.

Upon oxidative formation of the disulfide bridge, the rate constant for fumarate reduction was 25% of the wild-type k_{cat} value, implying that formation of the disulfide bridge is further hindering fumarate reduction.

The pH activity profile for wild-type flavocytochrome c_3 is shown in Figure 3. This shows that maximum turnover rates occur at lower pH values and decrease with increasing pH. The observed pK_a of 7.5 (±0.1) has been attributed to an active site histidine, His504 (*12*). The pH activity profile for the A251C:S430C double mutant enzyme is a bell-shaped curve that appears to fit two pK_a values. While the higher pK_a is definable, the lack of data at low pH values prevents the resolution of the lower pK_a value. The measured pK_a values for fumarate reduction with the disulfide in both the bridged and the nonbridged forms are essentially identical, at 8.2 (±0.1) with the disulfide open and 8.6 (±0.1) with the disulfide bridge (Figure 3).

Solvent−Kinetic−Isotope Effects. The deuterium solvent−kinetic−isotope effects of wild-type (*24*) and A251C:S430C double mutant forms of flavocytochrome c_3 have been determined over a range of pL values. It is apparent that there is essentially no difference between the effects exhibited by the double mutant when the disulfide bridge is oxidized and by the wild-type enzyme (Table 2). In the wild-type

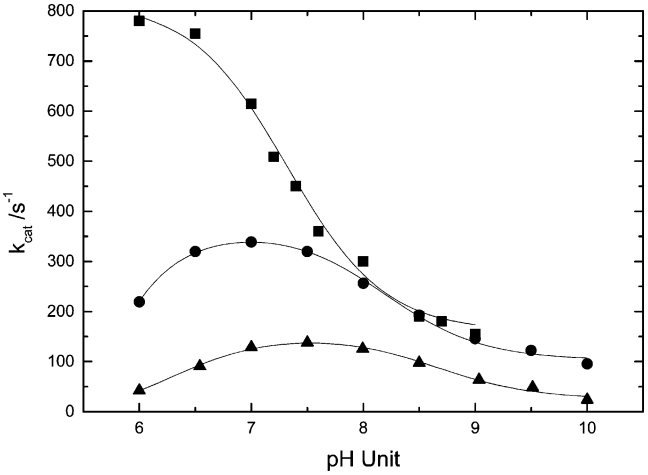

FIGURE 3: pH dependence of fumarate reductase activity under substrate-saturating conditions (1 mM fumarate, 25 °C, $I = 0.5$ M). Data shown are for wild-type enzyme (■), A251C:S430C with the disulfide open (●), and A251C:S430C with the disulfide bridged (▲).

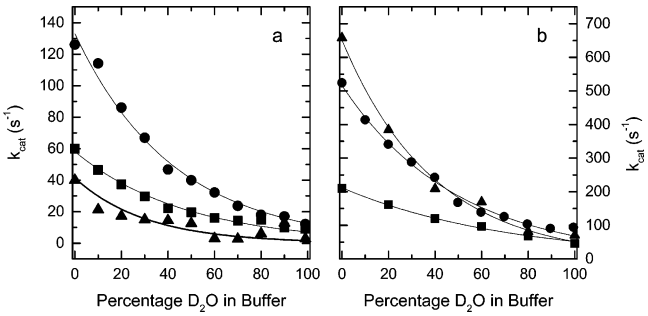

FIGURE 4: Proton inventory curves showing the effect on k_{cat} upon partial and complete deuteration of the assay buffer for (a) A251C:S430C flavocytochrome c_3 and (b) wild-type flavocytochrome c_3. All assays were carried out at 25 °C, $I = 0.5$ M, and under saturating fumarate conditions (1 mM). In the double mutant enzyme, the disulfide bridge is formed. Proton inventories were constructed at pL values 6.0 (▲), 7.2 (●), and 9.0 (■) and fitted to a model corresponding to multiple hydrogenic sites in reactant and transition states, as described by Schowen and Schowen (*20*). Solvent isotope effects were calculated as k_H/k_D and are outlined in Table 2.

Table 2: Deuterium Solvent−Kinetic−Isotope Effects for Wild-Type and A251C:S430C Flavocytochromes c_3 (25 °C, $I = 0.5$ M, fumarate − 1 mM)

	k_H/k_D	
pL	wild-type	A251C:S430C
6.0	13 ± 2	13.7 ± 2.5
7.2	8.2 ± 0.4	10.1 ± 1.5
9.0	4.0 ± 0.3	6.7 ± 1.6

enzyme, fumarate turnover is believed to be rate-limited by the delivery of protons to the active site (*15*, *25*), and this is reflected in the large solvent isotope effects calculated. The close similarity between both the solvent−kinetic−isotope effects observed and the proton inventory curves obtained (Figure 4) for the disulfide-bridged double mutant enzyme and the wild-type enzyme would suggest that proton and/or hydride delivery is rate-limiting in both and that the same proton delivery pathway is in operation in both forms of the enzyme.

Presteady State Kinetic Analysis. The course of fumarate-dependent heme reoxidation was monitored at 418 nm by stopped-flow analysis. All of the results quoted were obtained

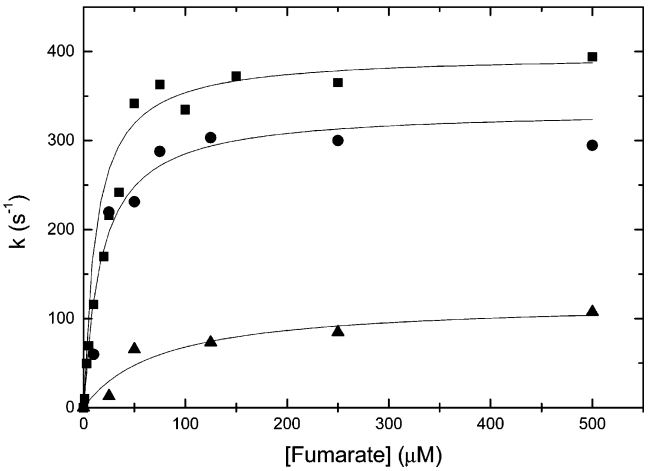

FIGURE 5: Presteady state reoxidation of the hemes of wild-type and A251C:S430C double mutant flavocytochrome c_3. Shown is the Michaelis−Menten curve for the fast phase of heme reoxidation (pH 7.2, 25 °C, $I = 0.5$ M). The slow phases of heme reoxidation have been omitted but are also decreased by a similar magnitude as a result of the substitutions. Data shown are for wild-type enzyme (■), A251C:S430C with the disulfide open (●), and A251C:S430C with the disulfide bridged (▲).

Table 3: Data Collection and Refinement Statistics

resolution (Å)	24.0−1.6
total no. of reflections	358 156
no. of unique reflections	77 814
completeness (%)	92.2
$I/[\sigma(I)]$	14.3
R_{merge} (%)[a]	5.8
R_{merge} in outer shell (1.66−1.60 Å) (%)	34.5
R_{cryst} (%)[b]	15.53
R_{free} (%)[b]	19.71
rmsd from ideal values	
bond lengths (Å)	0.013
bond angles (deg)	1.5
Ramachandran analysis	
most favored (%)	87.3
additionally allowed (%)	12.5

[a] $R_{merge} = \Sigma_h\Sigma_i|I(h) - I_I(h)|/\Sigma_h\Sigma_i I_I(h)$, where $I_I(h)$ and $I(h)$ are the ith and mean measurement of reflection h, respectively. [b] $R_{cryst} = \Sigma_h|F_o - F_c|/\Sigma_h F_o$, where F_o and F_c are the observed and calculated structure factor amplitudes of reflection h, respectively. R_{free} is the test reflection data set, 5% selected randomly for cross-validation during crystallographic refinement.

at pH 7.2. The data obtained for the recombinant wild-type enzyme show a maximal heme reoxidation rate of 400 s^{-1} (*15*). The rate of heme reoxidation in the A251C:S430C double mutant enzyme was measured in both the presence and the absence of DTT (Figure 5). In the presence of DTT, Ellman assay analysis confirmed the absence of the disulfide bridge and the rate constant for heme reoxidation was determined to be 335 ± 28 s^{-1}, 84% of the value for the wild-type enzyme. Formation of the disulfide bridge decreased the rate constant for heme reoxidation to 119 ± 18 s^{-1}, some 35% of the rate in the DTT-reduced enzyme and 30% of the rate in the wild-type enzyme. The magnitude of the rate constants obtained is in accordance with the data obtained under steady state conditions.

Crystal Structure of A251C:S430C Flavocytochrome c_3. A data set to 1.6 Å resolution was used to refine the structure to a final *R*-factor of 15.53% (R_{free} = 19.71%) (Table 3). The final model consists of one protein molecule, comprising residues 1−568, four hemes, the FAD, one substrate-like molecule, and one sodium ion. In addition, there are 1228 water molecules. Three residues at the C terminus of the protein (residues 569−571) could not be located in the electron density map. The rmsd fit of all backbone atoms for the wild-type and A251C:S430C enzymes is 0.2 Å, indicating no major differences between the two structures.

Interestingly, although both wild-type and A251C:S430C enzymes were crystallized in the presence of fumarate, the molecule found at the active site is a C2-hydroxylated derivative of fumarate. A mechanism for the formation of this hydroxylated substrate has been proposed (*8*), and it is assumed that such a mechanism is responsible for the observation of the same molecule in the same twisted conformation in the structure of the A251C:S430C enzyme. The exact identity of the species bound at the active site has been investigated by the recent solution of the crystal structures of the wild-type enzyme with both L- and D-malate present at the active site, but at the resolution of the data obtained, it is impossible to distinguish which enantiomer is formed from fumarate in the crystal (or indeed whether both may be present) (unpublished results).

Comparison of the structures of the wild-type and A251C:S430C enzymes reveals that the only significant difference between the two structures lies in the formation of a disulfide bond between the two cysteine residues introduced by site-directed mutagenesis (Figure 6a). From Figure 6b, it can be seen that introduction of the disulfide bond has little effect on the position of the protein backbone around the site of the substitution, and in fact, the result of the formation of the disulfide bond is that the clamp domain is tethered in exactly the same position as it is observed in the wild-type enzyme structure solved by Taylor et al. (*8*; PDB ID 1QJD).

DISCUSSION

To investigate the role of domain mobility in flavocytochrome c_3 (and fumarate reductases in general), we have attempted to restrict such movement by the introduction of a covalent bond between the FAD-binding and clamp domains. Several publications have mentioned the potential importance of clamp domain mobility in catalysis. For example, the structure of one of the *S. frigidimarina* fumarate reductase isozymes [Ifc$_3$; 1QO8 (*9*)] has been solved in a ligand-free open conformation, and a role in modulation of substrate access has been proposed for the mobile clamp domain. Further evidence for domain mobility comes from the structure of the *W. succinogenes* fumarate reductase (*5*, *6*; PDB ID 1QLB and 1E7P), which has been solved in three different crystal forms yielding two distinct structures. In one of these, the clamp domain is positioned in an "open", inactive conformation (1QLB), and in the other (1E7P), there is a 14° movement of the clamp domain relative to the FAD-binding domain when compared to that observed in the open conformation. It is this closed conformation that more closely resembles the majority of fumarate reductase/succinate dehydrogenase structures available. In fact, when all of these available structures are overlaid, a comparison of the position of the α-carbon of the active site arginine reveals that all are within 2 Å of the α-carbon of Arg402 of 1QJD except that of the open conformation of the *W. succinogenes* enzyme (Arg301; 3.43 Å) and that of the open conformation of the *S. frigidimarina* isozyme (1QO8) (R397; 6.72 Å). Such structural information would inevitably lead to the conclusion

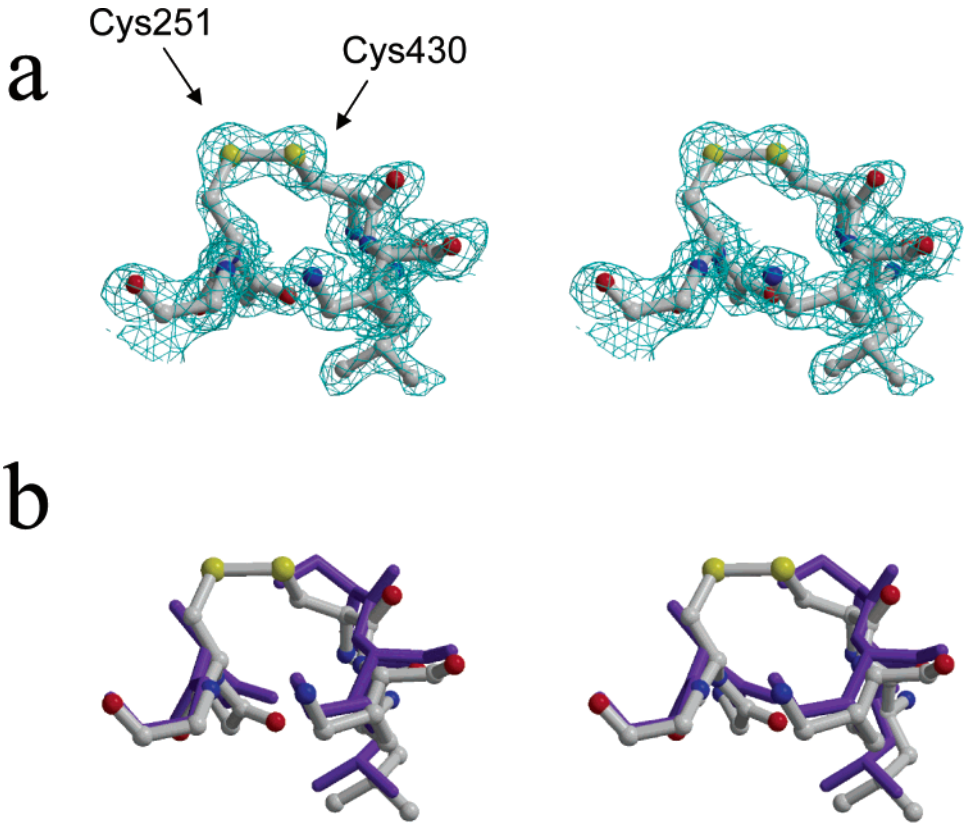

FIGURE 6: (a) Stereoview of the region surrounding the disulfide bond formed between Cys251 and Cys430 in the A251C:S430C double mutant flavocytochrome c_3. Residues shown are Gly250, Cys251, Gly252, Leu429, Cys430, and Lys431. The electron density map was calculated using Fourier coefficients $2F_o - F_c$, where F_o and F_c are the observed and calculated structure factors, respectively, the latter based on the final model. The contour level is 1σ, where σ is the rms electron density. (b) Stereo overlay of the same region with that of the wild-type structure (purple). Minimal movement of the protein backbone is observed as a result of the substitutions and disulfide bond formation. This figure was generated using BOBSCRIPT (*26*) and RASTER 3D (*27*).

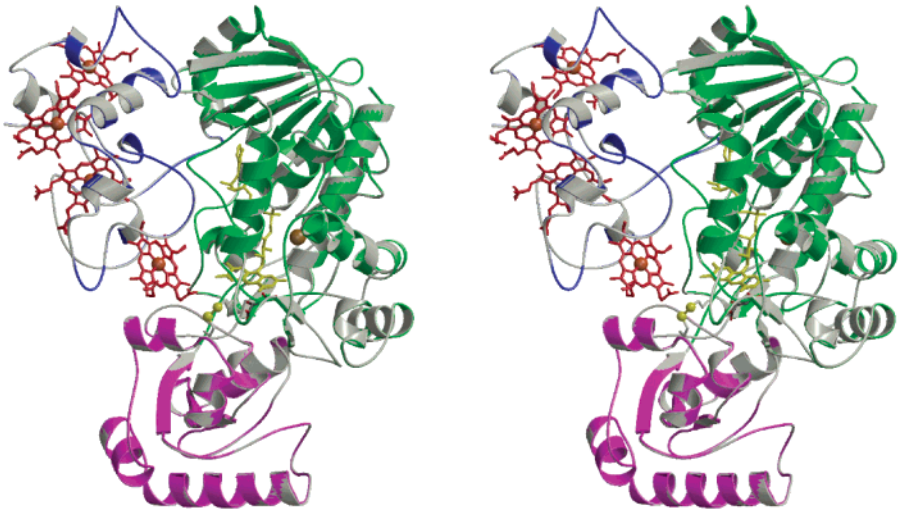

FIGURE 7: Stereoview of the overlaid structures of the wild-type and A251C:S430C double mutant flavocytochromes c_3. The domain structure of the wild-type enzyme is highlighted, with the heme domain in blue, the FAD-binding domain in green, and the clamp domain in magenta. The double mutant enzyme is shown in gray, and the position of the disulfide bond is illustrated. It can be seen that the two structures are completely superimposable. This figure was generated using BOBSCRIPT (*26*) and RASTER 3D (*27*).

that some movement of the clamp domain is necessary to allow access of substrate to the active site and that opening and closing of the active site in this way is an integral part of the catalytic cycle of the enzyme. Ala251 and Ser430 were chosen for substitution by cysteine in order to achieve an interdomain disulfide bond due to their relative positions in the flavin-binding and clamp domains, respectively. In addition, they had favorable side chain orientations with respect to each other. By comparison of the structure of the closed, substrate-bound flavocytochrome c_3 (*8*; PDB ID 1QJD) with that of the open, substrate-free isozyme (*9*; PDB ID 1QO8), it can be seen that while Ala251 and Ser430 are close enough to allow potential disulfide bond formation in the A251C:S430C double mutant enzyme (the α-carbon atoms are 4.7 Å apart), the distance between these atoms of the equivalent residues in the substrate-free isozyme (Lys246

and Lys425) is some 17.3 Å. Thus, it is clear that the location chosen for the disulfide bond is one where there is structural evidence for domain mobility. The crystal structure of the A251C:S430C double mutant flavocytochrome c_3 clearly shows the existence of a disulfide bond between the two engineered cysteine residues, a result which is corroborated by the results of Ellman assays, which confirm the presence of two free cysteine residues in the DTT-reduced enzyme and no free cysteine residues in the air-oxidized, disulfide-bridged enzyme. Steady state kinetic experiments indicate that the introduction of the two cysteine residues has the effect of decreasing the value of k_{cat} in the DTT-reduced enzyme to 63% of the value for wild-type enzyme, while in the oxidized disulfide-bridged form this value drops further, to approximately 25% of the wild-type value. Notably, there is little change in the value of K_M for fumarate binding as a result of the substitutions, indicating that fumarate binding at the active site is unaffected. Pre-steady-state kinetic analysis indicates a similar magnitude of decrease in the rate of fumarate-dependent heme reoxidation in both the DTT-reduced and the disulfide-bridged double mutant enzyme relative to the wild-type enzyme. It has been proposed that in the wild-type enzyme proton and/or hydride delivery to fumarate is the rate-limiting step in the catalytic cycle (*15*, *25*). Determination of solvent−kinetic−isotope effects for the wild-type and A251C:S430C enzymes displays no erosion of the solvent−kinetic−isotope effect as a result of disulfide formation in the mutant form, leading to the conclusion that rate limitation remains dependent upon this process.

It is clear from inspection of the structure of the A251C:S430C double mutant overlaid with that of the wild-type enzyme (Figure 7) that the enzyme structures are essentially identical when the disulfide bond is formed. It is, however, possible that in the nonbridged state the steric bulk of the side chain sulfur atoms of Cys251 and Cys430 prevents adoption of the exact conformation observed in the wild-type structure in terms of the relative positions of the FAD-binding and clamp domains. In this way, it is possible that proton delivery may be compromised by the double substitution thus resulting in the decreased k_{cat} value observed in the nonbridged form of the double mutant enzyme. Once the disulfide bond is formed, however, the relative positions of the FAD-binding and clamp domains are fixed such that the proposed proton pathway residues (Glu378, Arg381, and the active site acid Arg402) are seen in exactly the same positions as observed in the wild-type enzyme. This being the case (at least in the crystal structure), then the possible reasons for the decreased rate of fumarate reduction in the A251C:S430C double mutant must be considered. The observed decrease in the k_{cat} for fumarate reduction in the mutant enzyme is comparatively small (a 4-fold decrease in A251C:S30C relative to the wild-type enzyme at pH 7.2). Indeed, even if k_{cat}/K_M values are compared as a measure of catalytic efficiency, then the greatest effect (observed at pH 6.0) of restricted domain mobility is an 11-fold decrease in enzymatic efficiency. Therefore, although results indicate that domain mobility is significant in fumarate reductase, it is not essential for catalytic function, and evidence from solvent−kinetic−isotope effects would indicate that the altered kinetic characteristics in the disulfide-bridged enzyme are due to a decrease in the rate of proton or hydride transfer to fumarate during catalysis.

CONCLUSION

It is apparent from these results that clamp domain mobility affects catalysis but is not critical for the regulation of substrate access/product removal, and it is probable that the altered kinetic characteristics in the oxidized mutant enzyme are a result of a perturbation of active site rearrangement during catalysis as a consequence of disulfide bond formation.

REFERENCES

1. Körtner, C., Lauterbach, F., Tripier, D., Unden, G., and Kröger, A. (1990) *Mol. Microbiol. 4*, 855−860.
2. Cecchini, G., Schröder, I., Gunsalus, E., and Maklashina, E. (2002) *Biochim. Biophys. Acta 1553*, 140−157.
3. Gordon, E. H. J., Pealing, S. L., Chapman, S. K., Ward, F. B., and Reid, G. A. (1998) *Microbiology 4*, 937−945.
4. Iverson, T. M., Luna-Chavez, C., Cecchini, G., and Rees, D. C. (1999) *Science 284*, 1961−1966.
5. Lancaster, C. R. D., Kröger, A., Auer, M., and Michel, H. (1999) *Nature 402*, 377−385.
6. Lancaster, C. R. D., Gross. R., and Simon, J. (2001) *Eur. J. Biochem. 268*, 1820−1827.
7. Yankovskaya, V., Horsefield, R., Törnroth, S., Luna-Chavez, C., Miyoshi, H., Léger, C., Byrne, B., Cecchini, G., and Iwata, S. (2003) *Science 299*, 700−704.
8. Taylor, P., Pealing, S. L., Reid, G. A., Chapman, S. K., and Walkinshaw, M. D. (1999) *Nat. Struct. Biol. 6*, 1108−1112.
9. Bamford, V., Dobbin, P. S., Richardson, D. J., and Hemmings, A. M. (1999) *Nat. Struct. Biol. 6*, 1104−1107.
10. Leys, D., Tsapin, A. S., Nealson, K. H., Meyer, T. E., Cusanovich, M. A., and Van Beeumen, J. J. (1999) *Nat. Struct. Biol. 6*, 1113−1117.
11. Kunkel, T. A., and Roberts, J. D. (1987) *Methods Enzymol. 154*, 367−382.
12. Doherty, M. K., Pealing, S. L., Miles, C. S., Moysey, R., Taylor, P., Walkinshaw, M. D., Reid, G. A., and Chapman, S. K. (2000) *Biochemistry 39*, 10695−10701.
13. Mowat, C. G., Moysey, R., Miles, C. S., Leys, D., Doherty, M. K., Taylor, P., Walkinshaw, M. D., Reid, G. A., and Chapman, S. K. (2001) *Biochemistry 40*, 12292−12298.
14. Michel, L. O., Sandqvist, M., and Bagdasarian, M. (1995) *Gene 152*, 41−45.
15. Pealing, S. L., Cheesman, M. R., Reid, G. A., Thomson, A. J., Ward, F. B., and Chapman, S. K. (1995) *Biochemistry 34*, 6153−6158.
16. Pealing, S. L., Lysek, D. A., Taylor, P., Alexeev, D., Reid, G. A., Chapman, S. K., and Walkinshaw, M. D. (1999) *J. Struct. Biol. 127*, 76−78.
17. Macheroux, P. (1999) in *Flavoprotein Protocols: Methods in Molecular Biology* (Chapman, S. K., and Reid, G. A., Eds.) Vol. 131, pp 1−7, Humana Press, Totowa, NJ.
18. Turner, K. L., Doherty, M. K., Heering, H. A., Armstrong, F. A., Reid, G. A., and Chapman, S. K. (1999) *Biochemistry 38*, 3302−3309.
19. Glascoe, P. K., and Long, F. A. (1960) *J. Phys. Chem. 64*, 188−191.
20. Schowen, K. B., and Schowen, R. L. (1982) *Methods Enzymol. 87*, 551−606.
21. Otwinowski, Z., and Minor, W. (1997) *Methods Enzymol. 276*, 307−326.
22. Roussel, A., and Cambillau, C. (1991) TURBO-FRODO, in *Silicon Graphics Geometry Partners Directory 86*, Silicon Graphics, Mountain View, CA.
23. Murshudov, G. N., Vagin, A. A., and Dodson, E. J. (1997) *Acta Crystallogr. D53*, 240−255.
24. Pankhurst, K. (2002) Ph.D. Thesis, University of Edinburgh.
25. Jones, A. K., Camba, R., Reid, G. A., Chapman, S. K., and Armstrong, F. A. (2000) *J. Am. Chem. Soc. 122*, 6494−6495.
26. Esnouf, R. M. (1997) *J. Mol. Graph. 15*, 132−134.
27. Merritt, E. A., and Murphy, M. E. P. (1994) *Acta Crystallogr. D50*, 869−873.

BI030261W